Journal of Solid State Chemistry **144,** 388–391 (1999)
Article ID jssc.1999.8175, available online at http://www.idealibrary.com on

Room Temperature Solid State Synthesis and Characterization of a New Chromium Thiophosphate $Cr_4(P_2S_6)_3$

Zhong-Le Huang,[1] Jing-Tai Zhao, Jin-Xiao Mi, Shao-Yu Mao, and Lan-Sum Zheng

Department of Chemistry, Xiamen University, Xiamen 361005, People's Republic of China

Received October 30, 1998; in revised form January 6, 1999; accepted January 8, 1999

A new chromium thiophosphate $Cr_4(P_2S_6)_3$ was synthesized by solid state reaction between $Na_4P_2S_6 \cdot 6H_2O$ and $CrCl_3 \cdot 6H_2O$ at room temperature rather than by the ceramic method. The product was characterized by means of XRD, Raman spectroscopy, and magnetic measurements. XRD shows that $Cr_4(P_2S_6)_3$, isostructural with $Ga_4(P_2S_6)_3$, crystallizes in the monoclinic system with $a = 0.8692(5)$ nm, $b = 0.7562(6)$ nm, $c = 0.8344(6)$ nm, and $\beta = 91.97(7)^\circ$. The Raman spectrum bears the characteristic peaks for the $P_2S_6^{4-}$ anion group. Magnetic susceptibility data reveal the existence of a d^3Cr^{3+} cation. These results correspond to the charge balance $Cr_4^{3+}(P_2^{4+}S_6^{2-})_3$. © 1999 Academic Press

I. INTRODUCTION

In the past two decades, considerable interest has been focused on the first-row transition metal hexathiodiphosphate $M_2P_2S_6$ (1) (M = Mn, Fe, Co, Ni, Zn) which has semiconducting two-dimensional phases and presents many novel properties such as two-dimensional magnetic behavior, strong anisotropy of conductivity, and charge density waves. These lamellar compounds may undergo intercalation–deintercalation reactions involving host–guest redox processes and the relevant intercalated materials may have many new original properties. For example, intercalated layered materials $Mn_{1.72}P_2S_6(DAMS)_{0.56}$ exhibit both large optical nonlinearity and magnetic ordering (2); lithium-intercalated $Ni_2P_2S_6$ shows the potential to function as a cathode in lithium batteries (1).

For elements preceding manganese, no corresponding $M_2P_2S_6$ analogue has been reported. In the case of vanadium, a nonstoichiometric layered phase $V_{1.56}P_2S_6$ (3) is formed with the charge balance $V^{2+}_{0.68}V^{3+}_{0.88}[\ ]_{0.44}P_2S_6$. For titanium, a three-dimensional phase TiP_2S_6 (4) is formed with a Ti^{4+} cation and $P_2S_6^{4-}$ as in the two-dimensional $M_2P_2S_6$ family. The case of chromium is somewhat special because of the great stability of Cr^{3+} with its spherical d^3 electronic configuration. This is why no $Cr_2^{2+}P_2S_6$ phase has been reported. Instead, a $Cr^{3+}PS_4$ (5, 6) compound has been found with a layer structure but with P^{5+} in an inslab tetrahedral site.

It is reasonable to expect metal-deficient compounds of the $M_2P_2S_6$ type with a M^{3+} cation, and $M^{3+}_{4/3}P_2S_6$ compounds were indeed obtained with M = Ga (7) and In (8, 9). Many efforts were made to obtain an isostructural $Cr_{4/3}[\ ]_{2/3}P_2S_6$ phase by the traditional high-temperature method but failed and resulted in another chromium thiophosphate CrP_3S_{9+x} ($x \approx 0.25$) (10) with the charge balance $Cr^{3+}P_3^{5+}S^{2-}_{8.75}(S_2)^{2-}_{0.25}$.

Soft chemistry syntheses have been widely applied to metal hexathiodiphosphate compounds (11). In this paper we report the successful synthesis of $M_{4/3}P_2S_6$ by a new synthetic route—room temperature solid state reaction—and the XRD, Raman, and magnetic characterization of the compound.

II. EXPERIMENTAL

1. *Reagents and Apparatus*

$CrCl_3 \cdot 6H_2O$ is an analytical pure grade and $Na_4P_2S_6 \cdot 6H_2O$ was prepared according to a literature method (12). The compositions of final products were checked via energy dispersive analysis in a JEOL 1000 CX scanning electron microscope operating at 15 kV. XRD patterns were recorded on a Rigaku Rotflex D/MAX-RC model X-ray diffractometer with Cu target ($K\alpha$, λ = 0.15406 nm) and a graphite monochromator. Raman spectra were obtained on a confocal microprobe Raman system Labram I from Dilor-France using the 632.8 nm line of an He–Ne ion laser for sample excitation; the resolution was 4 cm^{-1} and the incident beam power on the samples was 5 mW. Magnetic measurements were carried out using a CF-1 model vibrating sample magnetometer (China–France) with H = 5 T in a temperature range of 1.5–300 K.

---

[1] To whom correspondence should be addressed. Fax: 0592-2188054 or 2186401. E-mail: zlhuang@jingxian.xmu.edu.cn.

0022-4596/99 $30.00

2. *Synthesis by Room Temperature Solid State Reactions and Analysis*

Accurately weighed $CrCl_3 \cdot 6H_2O$ (green crystal) and $Na_4P_2S_6 \cdot 6H_2O$ (white powder) in a 4 : 3 molar ratio were mixed and ground in an agate mortar to get the best possible homogeneity. The color of the mixture immediately turned from white and green to dark brown at room temperature. After one hour's grinding, a portion of the products was taken out to do XRD and the rest was washed with distilled water and anhydrous alcohol to remove NaCl. The dark brown products thus obtained were first dried under vacuum at room temperature and then annealed in an evacuated silica tube (1.3×10^{-2} Pa N_2 atmosphere) at different temperatures and at different time intervals.

Using $AgCrP_2S_6$ as a standard, semiquantitative chemical analysis by energy dispersive analysis gave an average Cr/P/S ratio of 1.35/2.03/5.7 for the sample before annealing and 1.34/2.02/5.8 for the calcined sample. These results showed that both the samples were homogeneous to within 3.0% in both chromium and phosphorus.

III. RESULTS AND DISCUSSION

1. *XRD Characterization*

The process of room-temperature solid state reaction between $CrCl_3 \cdot 6H_2O$ and $Na_4P_2S_6 \cdot 6H_2O$ and the heat treatment of reaction products were monitored by XRD. Figure 1 shows the XRD patterns for the reactant species before reaction, the products after reaction, and the final products at different annealing stages. From Figs. 1a–1e, one can see that 1 h of grinding is enough to complete the reaction; i.e., the $CrCl_3 \cdot 6H_2O$ and $Na_4P_2S_6 \cdot 6H_2O$ diffraction peaks disappear completely and new sharp diffraction peaks for NaCl appear. After removal of NaCl by washing with distilled water and anhydrous alcohol and drying under vacuum, a *no-peak* diffraction pattern is observed, (Fig. 1d) indicating the amorphous state for the product $Cr_4(P_2S_6)_3$. This implies that the concerned reaction occurs in the following manner:

$$4CrCl_3 \cdot 6H_2O + 3Na_4P_2S_6 \cdot 6H_2O \rightarrow Cr_4(P_2S_6)_3 + 12NaCl + 42H_2O.$$

The annealing of the products at 400°C for 24 h (1.3×10^{-2} Pa N_2 atmosphere) leads to the appearance of a broad diffraction peak around $2\theta = 14.5°$ (Fig. 1e), implying the beginning of crystallization and a nanometer size scale for the product particles. The annealing of the products at 500°C for 24 h (1.3×10^{-2} Pa N_2 atmosphere) yields a set of relatively sharp X-ray diffraction peaks with a characteristic strong reflection at $2\theta = 14.58°$ (Fig. 1f), evidencing the crystalline state of the final product $Cr_4(P_2S_6)_3$ (The average crystal size according to the Scherrer formula is 75 nm). The formation of $Cr_4(P_2S_6)_3$ thus occurs as follows:

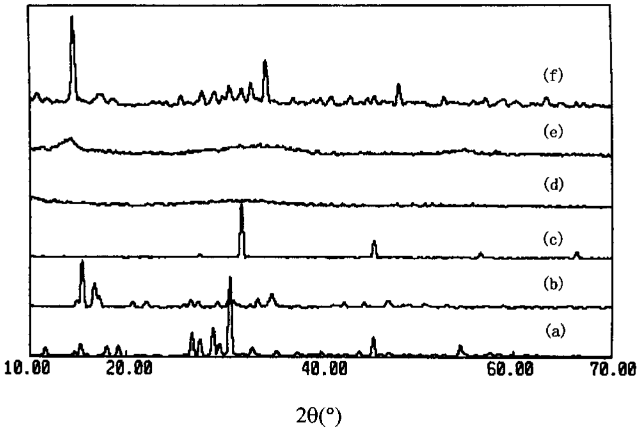

FIG. 1. XRD patterns for the room temperature solid state reaction between $CrCl_3 \cdot 6H_2O$ and $Na_4P_2S_6 \cdot 6H_2O$. (a) $Na_4P_2S_6 \cdot 6H_2O$; (b) $CrCl_3 \cdot 6H_2O$; (c) reaction products, amorphous $Cr_4(P_2S_6)_3$ and crystalline NaCl after 1 h of grinding; (d) reaction products, amorphous $Cr_4(P_2S_6)_3$ after removal of NaCl; (e) $Cr_4(P_2S_6)_3$ after annealing at 400°C for 24 h (1.3×10^{-2} PaN_2); (f) crystalline $Cr_4(P_2S_6)_3$ after annealing at 500°C for 24 h (1.3×10^{-2} Pa N_2).

$$\text{Crystalline reactant species} \xrightarrow{\text{reaction}} \text{amorphous } Cr_4(P_2S_6)_3 \xrightarrow{\text{annealing}} \text{crystalline } Cr_4(P_2S_6)_3$$

Other manners of annealing were also adopted but no improvement of the diffraction pattern was obtained. The XRD pattern of $Cr_4(P_2S_6)_3$ after annealing at 500°C for 24 h was therefore chosen to do the indexing.

Upon comparing the XRD patterns of $Cr_4(P_2S_6)_3$ with those of $Ga_4(P_2S_4)_3$ (7), $CrPS_4$ (5, 6) CrP_3S_{9+x} ($x \approx 0.25$) (10), and $In_4(P_2S_6)_3$ (8, 9), we find that the patterns for $Cr_4(P_2S_6)_3$ and $Ga_4(P_2S_6)_3$ resemble each other the most. The indexing for the title compound was thus based on the lattice parameters for $Ga_4(P_2S_6)_3$ ($a = 1.1842$ nm, $b = 0.7786$ nm, $c = 0.8289$ nm, $\beta = 133.41°$). The newly obtained lattice parameters after a least-squares refinement are $a = 1.184(4)$ nm, $b = 0.7567(7)$ nm, $c = 0.834(3)$ nm, $\beta = 132.8(2)°$. The lattice parameters given in Table 1 are crystallographically equivalent to the former but with the beta angle less than 120° after transformation. The observed d values are consistent with the calculated ones.

Considering the great stability of chromium (III) with octahedral sulfur coordination, we propose that $Cr_4(P_2S_6)_3$, the crystal structure of which has not been reported to our knowledge, is a metal-deficient hexathiodiphosphate (IV) like $In_4(P_2S_6)_3$ and $Ga_4(P_2S_6)_3$ with

TABLE 1
X-Ray Powder Diffraction Data for $Cr_4(P_2S_6)_3$

d_{obs} (nm)	d_{calc} (nm)	h	k	l	I/I_0
0.6101	0.6121	− 1	0	1	100
0.3469	0.3471	− 2	1	1	14
0.3200	0.3217	− 1	2	1	18
0.3056	0.3060	− 2	0	2	17
0.2910	0.2896	3	0	0	23
0.2800	0.2800	0	2	2	21
0.2717	0.2717	− 2	2	1	26
0.2602	0.2597	− 3	1	1	53
0.2188	0.2183	− 1	2	3	11
0.2090	0.2087	4	1	0	13
0.2011	0.2011	1	0	4	10
0.1982	0.1990	3	2	2	12
0.1885	0.1883	− 4	2	0	24
0.1729	0.1729	− 2	3	3	11
0.1643	0.1643	4	1	3	8
0.1607	0.1607	0	3	4	9
0.1559	0.1560	− 5	2	1	7
0.1465	0.1465	1	5	1	10

Note. $a = 0.8692(5)$ nm, $b = 0.7562(4)$ nm, $c = 0.8344(6)$ nm, $\beta = 91.97(7)^\circ$. The indexing was based on the lattice parameters for $Ga_4(P_2S_6)_3$ (7). The average $\Delta(2\theta)$ (theo. − exp.) is 0.056°.

layer structure and can be described as $Cr_{1.33}[\ ]_{0.67}P_2S_6$. Its crystal structure would be expected to be built from a close packed stacking of sulfur ions with the chromium (III), phosphorus–phosphorus pairs (P_2), and the vacancies occupying the octahedral sites between the sulfur layers. The two related chromium(III) ternary thiophosphates are $CrPS_4$ (5, 6), with a layered structure but with P(V) in inslab tetrahedral sites, and CrP_3S_{9+x}($x \approx 0.25$) (10), with an interlocked structure made of three independent networks. The common point for the structures of these ternary thiophosphates lies in the great stability of chromium(III) with octahedral sulfur coordination.

2. *Raman Spectra*

Raman spectra for $Na_4P_2S_6 \cdot 6H_2O$ and reaction products $Cr_4(P_2S_6)_3$ after removal of NaCl are shown in Fig. 2. These two sets of spectra resemble each other and all bear the characteristic peaks for the anion group $P_2S_6^{4-}$ where the broadened ones for $Cr_4(P_2S_6)_3$ might be attributed to its amorphous state. Symmetry analysis for $P_2S_6^{4-}(D_{3d})$ symmetry gives the following modes: $\Gamma_{vib}(D_{3d}) = 3A_{1g}(R) + 3E_g(R) + A_{1u} + 2A_{2u}(IR) + 3E_u(IR)$. Based on the assignment of the Raman bands for the hexathiodiphosphates (13), the peaks above 150 cm^{-1} correspond principally to the modes of the $P_2S_6^{4-}$ unit, whereas the peaks below 150 cm^{-1} might be assigned to the modes with the participation of metal ions. The most intense peak at 377 cm^{-1} for $Na_4P_2S_6 \cdot 6H_2O$ and 381 cm^{-1} for $Cr_4(P_2S_6)_3$ are the mixed symmetric P–P and P–S stretching modes (A_{1g}), while the strong and broad bands in the 150–350 cm^{-1} could be assigned to the P_2S_6 deformation vibrations (S–P–S and S–P–P modes (E_g). The shift of the corresponding peaks between $Na_4P_2S_6 \cdot 6H_2O$ and $Cr_4(P_2S_6)_3$ spectra signifies a change in the structural environment of the $P_2S_6^{4-}$ anion before and after the reaction. It also evidences the occurrence of the room-temperature solid state reaction between $Na_4P_2S_6 \cdot 6H_2O$ and $CrCl_3 \cdot 6H_2O$.

3. *Magnetic Properties*

Susceptibility measurements were carried out on a CV-1 model vibrating sample magnetometer in the 1.5–300 K temperature range with $H = 5$ T. Only a powder sample after annealing at 500°C for 24 h was studied. Figure 3 shows the temperature dependence of the magnetic susceptibility (χ_{mol}) and inverse magnetic susceptibility ($1/\chi$). Curie–Weiss behavior described by $1/\chi_{mol} = (T - \theta_P)/C_{mol}$ (where C_{mol} and θ_P are the molar Curie constant and the Weiss constant, respectively) is found in the high temperature range (50–300 K) with Curie constant $C_{mol} = 1.64$ and Bohr magneton $\mu_{exp} = 2.828(C_{mol})^{1/2} = 3.62\ \mu_B$. This is in good agreement with the calculated spin only value for Cr^{3+} ions ($C_{mol} = 1.87$ and $\mu_{calc} = 3.87\ \mu_B$ for spin only d^3). The Weiss constant is very weak and negative ($\theta_P = -3K$); that is, the magnetic interactions are weak and of the antiferromagnetic type. Similar antiferromagnetic orderings are observed for $CrPS_4^{(14)}$, PCr_5Se_{10} (15), and CrP_3S_{9+x} ($x \approx 0.25$) (10). The diamagnetic corrections have been done after the standard diamagnetic core contributions. The corresponding charge balance is thus $Cr_4^{3+}(P_2^{+4}S_6^{2-})_3$.

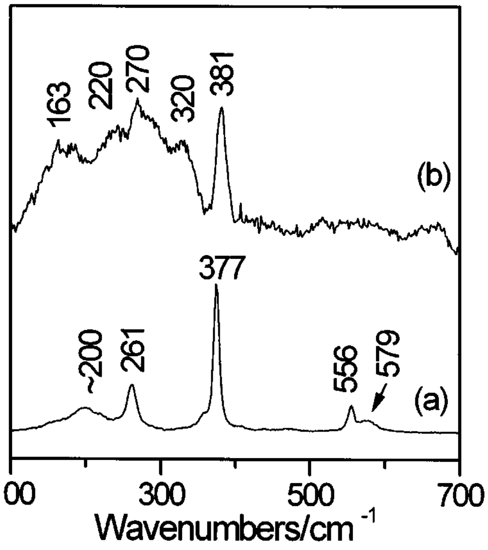

FIG. 2. Raman spectra: (a) $Na_4P_2S_6 \cdot 6H_2O$; (b) reaction products, $Cr_4(P_2S_6)_3$ after removal of NaCl.

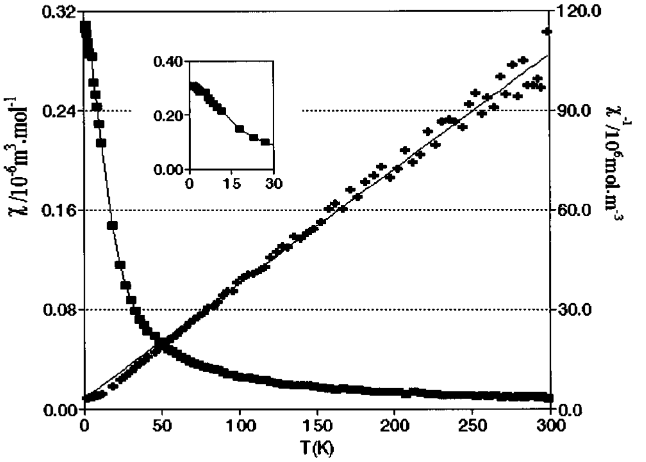

FIG. 3. $Cr_4(P_2S_6)_3$. Magnetic susceptibility and inverse susceptibility curves.

ACKNOWLEDGMENT

The Project is sponsored by the Scientific Research Foundation for Returned Overseas Chinese Scholars and Postdoctors, State Education Commission of China.

REFERENCES

1. R. Brec, *Solid State Ionics* **22,** 3 (1986).
2. P. G. Lacroix, R. Clement, and K. Nakatani, *Science* **263,** 658 (1994).
3. G. Ouvrard, R. Freour, R. Brec, and J. Rouxel, *Mater. Res. Bull.* **20,** 1053 (1985).
4. M. Z. Jandali, G. Eulenberger, and H. Hahn, *Z. Anorg. Allg. Chem.* **470,** 39 (1980).
5. P. Toffoli, P. Khodadad, and N. Rodier, *Acta Crystallogr. B* **33,** 285 (1977).
6. R. Diel and C. D. Carpentier, *Acta Crystallogr. B* **33,** 1399 (1977).
7. D. S. Kyriakos, A. N. Anagnostopoulos, P. Christidis, and V. Gountsidou, *J. Cryst. Growth* **76,** 6 (1986).
8. S. Soled and A. Wold, *Mater. Res. Bull.* **11,** 657 (1976).
9. A. Bubenzer, R. Nitsche, and A. Raufer, *J. Cryst. Growth* **29,** 237 (1975).
10. P. Fragnaud, M. Evain, E. Prouzet, and R. Brec, *J. Solid State Chem.* **102,** 390 (1993).
11. See for example: C. Gledel, JP. Audiere, R. Clement, and R. Cortes, *J. Chem. Phys. Physico-Chem. Biol.* **86,** 1692 (1989); X. Bourdon, E. Prouzet, and V. B. Cajipe, *J. Solid State Chem.* **129,** 157 (1997). E. Prouzet, G. Ouvrard, R. Brec, and P. Seguineau, *Solid State Ionics* **31,** 79 (1988).
12. H. Falius, *Z. Anorg. Allg. Chem.* **356,** 189 (1968).
13. See for example: Grzechnik, V. B. Cajipe, C. Payen, and P. F. McMillan, *Solid State Commun.* **108,** 43 (1998); W. Brockner and U. Patzmann, *Z. Naturforsch.* **38a,** 92 (1983); Z. L. Huang, "Contribution to the Study of Rare Earth Thiophosphates: Structure and Physical Properties," thesis, University of Nantes, France, 1994; C. Sourisseau, J. P. Forgerit, and Y. Mathey, *J. Solid State Chem.* **49,** 134 (1983); R. Becker and W. Brockner, *Z. Naturforsch.* **38a,** 874 (1983); B. Scott, M. Pressprich, R. D. Willet, and D. A. Cleary, *J. Solid State Chem.* **96,** 294 (1992).
14. A. Louisy, G. Ouvrard, D. M. Schleich, and R. Brec, *Solid State Commun.* **28,** 61 (1978).
15. R. Brec, A. Louisy, G. Ouvrard, A. Verbaere, and J. Rouxel, *Rev. Chim. Miner.* **19,** 49(1982).